Effects of acetone-soaking treatment on the performance of polymer solar cells based on P3HT/PCBM bulk heterojunction*

Liu Yu-Xuan(刘宇譞)[a], Lü Long-Feng(吕龙峰)[a], Ning Yu(宁 宇)[a], Lu Yun-Zhang(陆运章)[a], Lu Qi-Peng(鲁启鹏)[a], Zhang Chun-Mei(张春梅)[a], Fang Yi(方 一)[a], Tang Ai-Wei(唐爱伟)[b], Hu Yu-Feng(胡煜峰)[a], Lou Zhi-Dong(娄志东)[a], Teng Feng(滕 枫)[a]†, and Hou Yan-Bing(侯延冰)[a]‡

[a] *Key Laboratory of Luminescence and Optical Information of the Ministry of Education; Institute of Optoelectronic Technology, Beijing Jiaotong University, Beijing* 100044, *China*

[b] *Department of Chemistry, School of Science, Beijing Jiaotong University, Beijing* 100044, *China*

(Received 25 February 2014; revised manuscript received 10 May 2014; published online 10 September 2014)

The improvement of the acetone-soaking treatment to the performance of polymer solar cells based on the P3HT/PCBM bulk heterojunction is reported. Undergoing acetone-soaking, the PCBM does not distribute uniformly in the vertical direction, a PCBM enrichment layer forms on the top of the active layer, which is beneficial to the collection of the carriers and blocking the inverting diffusion carriers. X-ray photoelectron spectroscopy (XPS) analysis reveals that the PCBM weight ratio on the top of the active layer increases by 20% after the acetone-soaking treatment. Due to the nonuniform distribution of PCBM, the short-circuit current density, the open-circuit voltage, and the fill factor are enhanced significantly. Finally, the power conversion efficiency of the acetone-soaking device increases by 31% compared with the control device.

Keywords: polymer solar cells, solvent treatment, vertical phase separation, morphology

PACS: 88.40.jr, 84.60.Jt, 64.75.St, 73.50.–h **DOI:** 10.1088/1674-1056/23/11/118802

1. Introduction

Polymer solar cells have recently attracted considerable attention in both academia and industry for their unique advantages of compatibility with lightweight flexible substrates, large area fabrication, high-throughput productivity, low manufacturing cost, and extensive material source.[1–3]

The most intensively studied device structure of the polymer solar cells is the bulk heterojunction (BHJ), blending conjugated polymers (electron donor) with soluble fullerene derivatives (electron acceptor).[4] Among the blended materials of conjugated polymers and fullerene derivatives, a poly (3-hexylthiophene) (P3HT) and [6,6]-phenyl-C61-butyric acid methyl ester (PCBM) system has been intensively investigated as a prototype polymer solar cell.[2] This is attributed to its high degree of crystallinity, high hole mobility, broad absorption spectrum, and suitable band gap.[5]

Numerous improved approaches have been developed to increase the power conversion efficiency (PCE) of P3HT/PCBM BHJ polymer solar cells, such as optimizing the morphology of the active layer,[6] adding a buffer layer,[7] changing the electrode material,[8] introducing a surface plasmon resonance,[9] and using the tandem structure.[10] Among these approaches, controlling the morphology of the P3HT/PCBM blend film is the most crucial way for achieving a good device performance.[1] An ideal morphology of the active layer requires nanoscale phase separation with a bicontinuous interpenetrating network, which not only can provide a large interface between electron donor and electron acceptor for efficient exciton dissociation, but also can offer continuous and independent charge transport channels for better charge transport.[11] The nanoscale phase separation consists of lateral phase separation and vertical phase separation, both of which should be optimized for satisfying the device operation.[12] The phase separation in the lateral direction has attracted more attention over the past ten years, and several process conditions and post-treatments have been proposed, such as choosing appropriate solvents,[13] varying the blend ratio of donors and acceptors,[14,15] slow drying of spin-coated films,[16] adding additives into the solution of the active layers,[17,18] thermal annealing,[19,20] and solvent vapor annealing.[21,22]

Besides, it is worth noting that the component distribution of the donor and the acceptor molecules along the vertical direction is also crucial. As is well known, holes are transported to the indium tin oxide (ITO) anode through the pathways of the electron donor materials while electrons are transported to the metal cathode along the network of the electron acceptor materials.[11] Consequently, an ideal vertical phase separation with the donor towards the anode and the accep-

*Project supported by the National Natural Science Foundation of China (Grant Nos. 61275175, 61177017, and 61377028) and the National Natural Science Foundation of China for Distinguished Yong Scholars (Grant No. 61125505).

†Corresponding author. E-mail: FTeng@bjtu.edu.cn

‡Corresponding author. E-mail: ybhou@bjtu.edu.cn

© 2014 Chinese Physical Society and IOP Publishing Ltd

tor towards the cathode is favorable for reducing the transport distance of holes and electrons, which then improves the ability of charge transportation. Furthermore, this distribution can effectively suppress the recombination of holes and electrons at the electrode (or buffer layer)/active layer interfaces and is beneficial for charge collection. Over the past few years, the vertical morphology of the P3HT/PCBM blend films has been investigated by variable-angle spectroscopic ellipsometry (VASE),[23,24] neutron reflectivity (NR),[25–27] X-ray reflectivity (XRR),[28] X-ray photoelectron spectroscopy (XPS),[4,11] and near-edge X-ray absorption fine structure spectroscopy (NEXAFS).[24,29,30] Most of the results demonstrate that P3HT with lower surface energy tends to segregate at the air/active layer interface and PCBM with higher surface energy inclines to enrich at the substrate/active layer interface, which could minimize the interfacial free energy.[31] These findings suggest that the spontaneous vertical phase segregation during spin-coating is unfavorable for the carrier collection and transportation in the regular structure device.

To optimize the vertical morphology, thermal annealing[1,5,30] and buffer layer applications[4,23,24,29] were first proposed by some researchers. Recently, solvent surface treatment methods were proposed for the sake of controlling the vertical phase separation. Li *et al.*[11] presented a methanol (CH_3OH)/carbon disulfide (CS_2) mixed solvent soaking approach to simultaneously optimize the lateral and the vertical nanoscale phase separations of the active layer, and obtained a better performance than the thermal annealed device. Yang *et al.*[2] fabricated high short-circuit current (J_{SC}) devices with ethylene glycol monomethyl ether (EGME) spin-coating treatment before the zinc oxide nanoparticles (ZnO NPs) or lithium fluoride (LiF) cathode buffer layer and the Al cathode depositions. They suggested that the high J_{SC} is attributed to the formation of a PCBM-rich superficial region induced by the EGME treatment. In this study, we introduce a new acetone-soaking treatment approach and demonstrate that this approach can control the vertical morphology of the P3HT/PCBM polymer cells, resulting in the enhancement of the efficiency.

2. Experimental details

The device was fabricated on an ITO-coated glass substrate with the following structure: ITO-coated glass substrate/PEDOT:PSS/ P3HT:PCBM/ Al. Poly(3-hexylthiophene) (P3HT, $M_w = 68000$ g/mol, regioregularity = 95%) was obtained from Rieke Metals Inc, and [6,6]-phenyl-C61-butyric acid methyl ester (PCBM) was purchased from the Nano-C company. The typical solution used in this study for the spin-coating active layer was prepared as follows. P3HT and PCBM were dissolved in chlorobenzene (Alfa Aesar, 95%) in a 1:0.8 w/w ratio to form a 27-mg/mL solution. The blend solution was stirred in a glove box filled with N_2 at 45 °C for 12 h.

The ITO-coated glass substrate was cleaned with detergent, deionized water, acetone, and ethanol in an ultrasonic treatment, and then dried with N_2. The surface of the ITO-coated glass substrate was treated by UV-ozone for 15 min. As an anode modulation layer, poly (3,4-ethylenedioxylenethiophene):polystyrene sulfonic acid (PEDOT:PSS, H.C.Stark) was spin-casted (3000 rpm) on the substrate with a thickness of 40 nm from the aqueous solution (after passing through a 0.22 μm filter). The substrate was dried at 140 °C for 20 min in air and then transferred into a glove box to complete the following steps. The P3HT:PCBM blend solution was spin-coated at 1500 rpm onto the top of the PEDOT:PSS layer, and baked at 80 °C for 10 min to remove the residual solvent. After that, the substrate was soaked in the acetone solvent for 15 s, and then the substrate was removed from the acetone and dried with N_2 immediately. Subsequently, thermal evaporation was used to deposit a 100 nm thick aluminium (Al) electrode onto the surface of the active layer in a vacuum of 4×10^{-4} Pa. Finally, thermal annealing was carried out at 150 °C on a hot plate for 30 min. The active area of the device was 0.04 cm^2.

The current density–voltage (J–V) characteristics of the device were measured by a computer-controlled Keithley 6430 source measure unit. An AM 1.5 xenon-lamp-based solar simulator (San-Ei Electric) with an intensity of 100 mW/cm^2 was used to provide the illumination. The external quantum efficiency (EQE) measurements were carried out using a solar cell QE/IPCE measurement system (Zolix solar cell scan100). An ultraviolet–visible (UV–Vis) absorption spectrophotometer (Shimadzu, UV-3101PC) was used to study the absorption of the blend film, which was prepared using the same method as that for device fabrication. X-ray photoelectron spectroscopy (XPS) was performed using an ESCALAB 250 XPS analysis system with a monochromated Al $K\alpha$ X-ray source. For the non-annealed films, the XPS measurement was directly performed without Al deposition. For the post-annealing films with Al deposition, the Al electrode was removed with a diluted aqueous solution of sodium hydroxide (NaOH) after thermal annealing. Then the exposed surface was rinsed with deionized water, dried with N_2, and measured by XPS.

3. Results and discussion

The J–V characteristics of the P3HT/PCBM polymer solar cells with and without acetone treatment are shown in Fig. 1, and the device parameters are summarized in Table 1. The corresponding data were measured under AM 1.5 illumination from a calibrated solar simulator with an irradiation in-

tensity of 100 mW/cm^2. As shown in Table 1, the device without acetone treatment shows a limited performance: the short-circuit current density (J_{SC}) is 7.88 mA/cm^2, the open-circuit voltage (V_{OC}) is 0.62 V, the fill factor (FF) is 55%, and the power conversion efficiency (PCE) is 2.70%. When acetone is used to modify the active layer, the PCE has a significant enhancement of 31% from 2.70% to 3.54% with simultaneous improvements in J_{SC} (8.46 mA/cm^2), V_{OC} (0.64 V), and FF (65%). It is a significant improvement for the P3HT/PCBM polymer solar cells, considering there is no cathode modification layer used in our experiments.

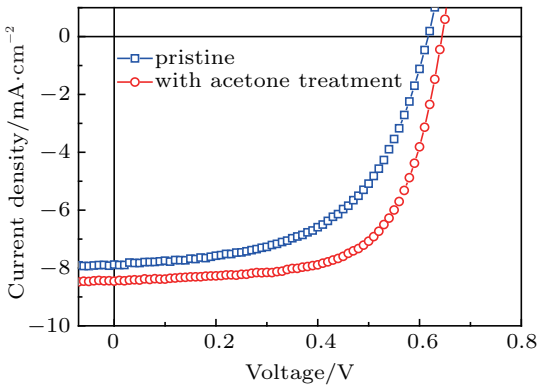


Fig. 1. (color online) The current density–voltage characteristics of solar cells based on P3HT/PCBM blends with and without acetone-soaking treatment under AM 1.5 illumination of intensity 100 mW/cm^2.

Table 1. Device performances of P3HT/PCBM blend solar cells with and without acetone-soaking treatment.

Treatment	J_{SC}/mA·cm^{-2}	V_{OC}/V	FF/%	PCE/%
None	7.88	0.62	55	2.70
Acetone	8.46	0.64	65	3.54

Figure 2 shows the results of external quantum efficiency (EQE) measurements for devices with and without acetone treatment. The EQE of the pristine device shows a maximum of 58% at the wavelength of 500 nm. On the other hand, for the device with acetone treatment, the EQE maximum increases to 60% at a wide wavelength range from 460 nm to 510 nm. Comparing the two curves, the obvious enhancement in the wavelength range of 390–600 nm after the acetone treatment contributes to the increases in J_{SC} and PCE of the device. The slight decrease in the wavelength range of 300–390 nm does not affect J_{SC} and PCE very much. As a consequence, the device with acetone treatment shows a stronger photoelectric response than the pristine one.

In polymer solar cells, the device performance strongly depends on the photoabsorption, exciton separation, charge transportation, and charge collection. The exciton dissociation rate in the BHJ structure is nearly 100%, so the enhancement of the device with acetone treatment could be attributed to the improvements in photoabsorption, carrier transportation, and carrier collection.

Figure 3 shows the UV–Vis absorption spectra of the blend films with and without acetone treatment. The absorption of P3HT around 500 nm does not change significantly after being soaked in the acetone solvent, which indicates that acetone has a negligible effect on P3HT. However, the absorption of PCBM around 330 nm decreases obviously without any shift in the wavelength. The previous reports showed that the absorption of PCBM changes and the maximum absorption wavelength of the PCBM molecules is almost constant when the amount of PCBM in the blend film is changed.[15] Therefore, the result in this test indicates the reduction of PCBM in the solvent treated active layer, which demonstrates the slow dissolution of PCBM in acetone. For the whole effective absorption wavelength range from 300 nm to 650 nm, the blend film with the acetone treatment does not exhibit any superiority in absorption intensity and even shows a lower absorption peak of PCBM than the pristine film. On the contrary, as shown in Fig. 2, the EQE increases obviously in the wavelength range from 390 nm to 600 nm and has a very slight decrease in the range of 300–390 nm. The comparison of Figs. 2 and 3 implies that the enhanced performance of the device soaked in acetone should be attributed to the charge carrier transportation and collection rather than the absorption.

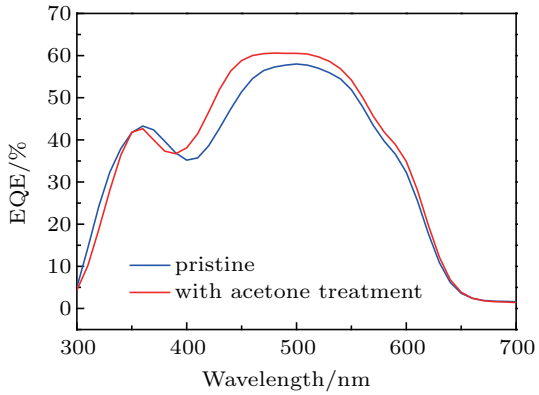


Fig. 2. (color online) The EQE spectra of solar cells based on P3HT/PCBM with and without acetone-soaking treatment.

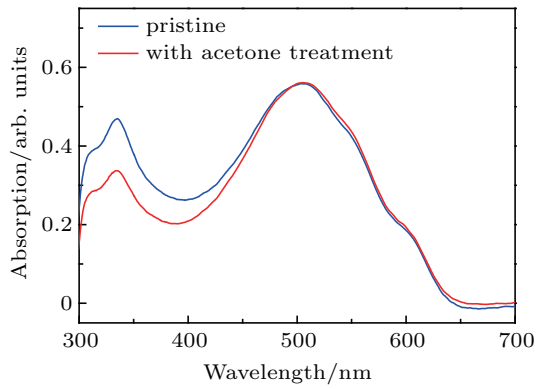


Fig. 3. (color online) UV–Vis absorption spectra of P3HT/PCBM blend films with and without acetone-soaking treatment.

In order to investigate the variation of the PCBM content in the active layer, X-ray photoelectron spectroscopy was used to measure the surface composition of the P3HT/PCBM blend film. From XPS, the weights and molar ratios of the components can be calculated from the peak intensities of the individual elements.[4] Because carbon exists in both P3HT and PCBM, the C (1s) atomic fraction represents the total content of P3HT and PCBM. Sulphur only exists in P3HT, so the S (2p) atomic fraction represents the content of P3HT. We can calculate the weight percentages of P3HT and PCBM at the active layer surface according to the atomic fractions of S (2p) and C (1s).

Table 2 summarizes the atomic fractions of C (1s) and S (2p) and the weight percentages of P3HT and PCBM for the surfaces under different treatments. As shown in the first two rows of Table 2, the non-annealed film was measured before the deposition of the Al electrode. For the surfaces without and with acetone treatment, the atomic ratios of C (1s) and S (2p) are very similar, which causes the almost equal P3HT ratios for non-treatment (89.26%) and acetone-treatment (89.02%) films. The high concentration of P3HT, which is nearly 90% at the top surface of the blend film, is attributed to the surface energy difference of the components. It is reported that P3HT shows a relatively lower surface energy (26.9 mJ/m^2) than PCBM (37.8 mJ/m^2),[3] and the surface composition changes to minimize the interfacial free energy.[31] Therefore, in order to reduce the free energy, P3HT inclines to accumulate on the top surface during spin-coating and forms a possible electron injection barrier. Similarly, the composition at the bottom surface of the active layer tends to be PCBM rich, creating a possible hole injection barrier.[29] So the enrichment of both P3HT and PCBM after spin-coating is adverse to the charge carrier transport and collection in the regular structure. Through some experiments, we find that PCBM has a low solubility in acetone while P3HT cannot dissolve in acetone, so the PCBM content in the acetone treated surface should decrease by the dissolution. However, the PCBM weight ratio of the acetone treated surface (10.98%) is close to that of the non-treatment surface (10.74%) in our result.

Table 2. Atomic and weight fractions at the top surfaces of P3HT/PCBM blend films without and with acetone-soaking treatment, before and after post-annealing at 150 °C for 30 min.

Annealing	Treatment	Atomic/%		Weight/%	
		C (1s)	S (2p)	P3HT	PCBM
None	none	92.05	7.95	89.26	10.74
	acetone	92.08	7.92	89.02	10.98
Post-anneal	none	95.70	4.30	51.76	48.24
	acetone	97.44	2.56	31.93	68.07

For the post-annealed film with Al deposition, the aqueous solution of sodium hydroxide (NaOH) was used to remove the Al electrode, and then the active layer was measured by XPS. This approach can provide us with the real composition of the surface under the Al electrode in the post-annealed device. In the last two lines of Table 2, the S (2p) atomic ratios of the post-annealed films (4.30% and 2.56%) are much lower than those of the non-annealed films (7.95% and 7.92%), which indicates that the proportion of P3HT:PCBM at the top surface is changed distinctly after post-annealing. The PCBM weight percentage of the film without solvent treatment increases from 10.74% to 48.24%. This could also be explained by the surface energy theory as follows: Al has a greatly higher surface energy ($> 10^3$ mJ/m^2)[32] than PEDOT:PSS (45.7 mJ/m^2),[11] PCBM with a relatively high surface energy is likely to diffuse to the Al electrode because of the surface energy inversion between the top surface and the bottom surface,[1] and the thermal annealing provides the driving force for the diffusion of PCBM. For the film undergoing both acetone treatment and post-annealing, the weight fraction of PCBM is further significantly increased to 68.07%, which indicates the aggravation of more PCBM on the top surface. Combined with the UV–Vis absorption results, which demonstrate the reduction of PCBM within the blend film, we can conclude that there exists a more suitable PCBM concentration gradient from a PCBM-poor bottom to a PCBM-rich top surface in the device with the acetone treatment active layer.

Such PCBM enrichment at the active layer/cathode interface would result in a desirable contact to extract electrons from PCBM and block hole diffusion from P3HT to the cathode effectively, which is beneficial to reduce the interface recombination of carriers and improve J_{SC}. The 0.02 V increase in V_{OC} for the acetone treated device could also be explained by this optimized vertical morphology. Normally, the V_{OC} of the device with a bilayer structure is higher than that of BHJ polymer solar cells because both electrons and holes can more easily be transported to an appropriate electrode without recombination.[33] In the BHJ structure, the vertical phase separation with PCBM-rich near the cathode and P3HT-rich near the anode is like a bilayer structure. Thus, the significant reduction in the reverse saturation current[1] and the remarkable increase in the shunt resistance[33] in this optimized vertical morphology would lead to improved V_{OC}. Furthermore, the significant 10% enhancement in FF suggests that the charge transport in the device is more balanced and the bicontinuous interpenetrating network structure is more ideal,[16] which is hard to be detected.

Summarizing all the results, we can outline the possible morphology evolution process of the P3HT/PCBM blend film under the collaboration of acetone-soaking treatment and thermal annealing. The schematic diagram is shown in Fig. 4. During spin-coating, P3HT inclines to accumulate on the top surface and PCBM tends to enrich on the bottom surface due

to the difference of the surface energy. When the blend film is soaked in acetone, the acetone dissolves the surface PCBM, and permeates into the blend film along some vertical pathways. The roadside PCBM dissolves in acetone and diffuses to the top surface because the outside concentration of PCBM is lower. Campoy-Quiles *et al.*[23] reported a PCBM concentration gradient increasing from the top surface to the bottom surface, so the inside PCBM could fill the vacancies on the top surface. Meanwhile, when the film dries with N_2, some PCBM may remain on the top surface with the evaporation of acetone. So the content of PCBM on the top surface after the acetone treatment does not change obviously in the XPS result. Although the surface composition is roughly the same after the acetone treatment and drying, some changes of the morphology within the film have taken place. After the deposition of Al with a fairly high surface energy, a surface energy inversion between the top and the bottom surfaces occurs. As small molecules, PCBM with higher surface energy inclines to diffuse from the bottom surface or the inside of the active layer to the top surface during thermal annealing. The acetone treatment makes PCBM easier to move along the acetone penetration pathways to the top surface of the active layer. Moreover, the aggregation of PCBM in these pathways could be improved so the interpenetrating network is more ideal. As a consequence, the acetone treatment accompanying thermal annealing optimizes both the electrode contact and the bicontinuous interpenetrating network, and improves J_{SC}, V_{OC}, and FF simultaneously compared with those of the regular post-annealing device.

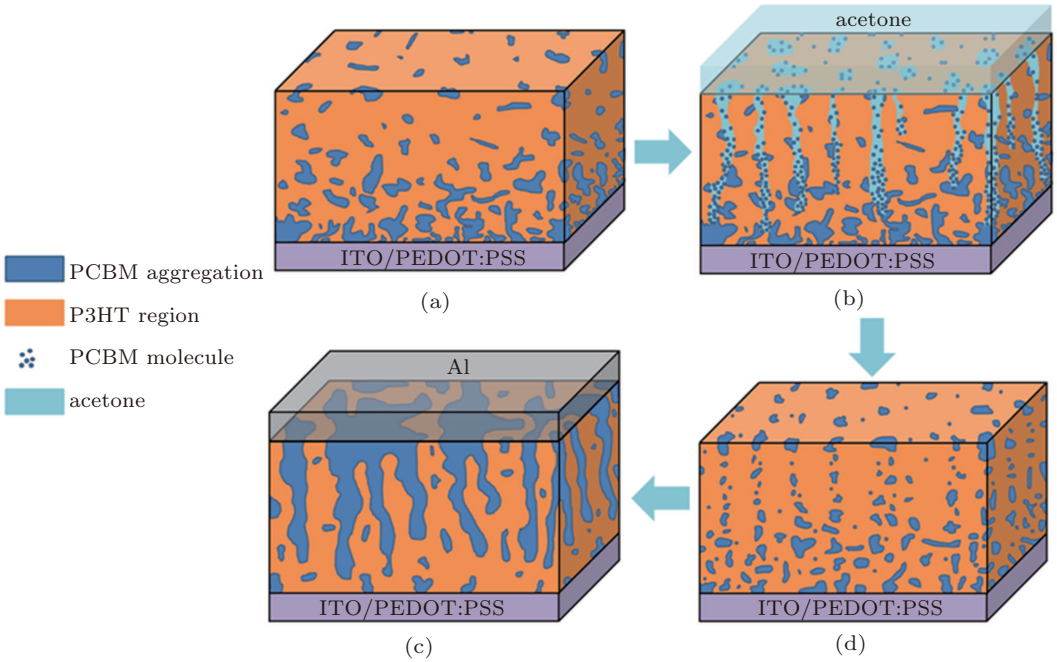


Fig. 4. (color online) Schematic diagram of morphology evolution of the P3HT/PCBM active layer soaked in acetone: (a) the pristine film, (b) the acetone treated film, (c) the dried film, and (d) the device with post-annealing.

4. Conclusion

We demonstrate a new solvent treatment approach to control the vertical distribution of PCBM in P3HT/PCBM composite films. The acetone-soaked device shows a significant enhancement in J_{SC}, V_{OC}, and FF. After optimization, the PCE of the acetone-soaking device increases by 31% compared with that of the control device. The EQE spectra and the UV–Vis absorption spectra indicate that the performance improvement of the acetone treated device should be attributed to the improvements in charge carrier transportation and collection. The XPS analysis reveals that the acetone treatment makes PCBM more easily diffuse from the bottom surface to the top surface during post-annealing, forming an ideal vertical phase separation with PCBM enriched on the top surface and a better bicontinuous interpenetrating network. This acetone-soaking treatment may provide a simple and effective approach to obtain high-performance BHJ polymer solar cells.

References

[1] Orimo A, Masuda K, Honda S, Benten H, Ito S, Ohkita H and Tsuji H 2010 *Appl. Phys. Lett.* **96** 43305
[2] Yang B, Tsai M, Cheng W, Chen J, Hsu S L and Chou W 2013 *J. Phys. Chem. C* **117** 14472
[3] Watts B, Belcher W J, Thomsen L, Ade H and Dastoor P C 2009 *Macromolecules* **42** 8392
[4] Xu Z, Chen L M, Yang G W, Huang C H, Hou J H, Wu Y, Li G, Hsu C S and Yang Y 2009 *Adv. Funct. Mater.* **19** 1227
[5] Oklobia O and Shafai T S 2013 *Sol. Energy Mater. Sol. Cells* **117** 1
[6] Lee J K, Ma W L, Brabec C J, Yuen J, Moon J S, Kim J Y, Lee K, Bazan G C and Heeger A J 2008 *J. Am. Chem. Soc.* **130** 3619
[7] Yu X, Hu Z Y, Huang Z H, Yu X M, Zhang J J, Zhao G S and Zhao Y 2013 *Chin. Phys. B* **22** 118801

[8] ReeseM O, WhiteM S, Rumbles G, Ginley D S and Shaheen S E 2008 *Appl. Phys. Lett.* **92** 53307

[9] Kim S, Na S, Jo J, Kim D and Nah Y 2008 *Appl. Phys. Lett.* **93** 73307

[10] Qing J, Zhong Z F, Liu Y, Li B J and Zhou X 2014 *Chin. Phys. B* **23** 038802

[11] Li H, Tang H W, Li L G, Xu W T, Zhao X L and Yang X N 2011 *J. Mater. Chem.* **21** 6563

[12] Chen L, Hong Z, Li G and Yang Y 2009 *Adv. Mater.* **21** 1434

[13] Kim Y, Choulis S A, Nelson J, Bradley D D, Cook S and Durrant J R 2005 *Appl. Phys. Lett.* **86** 63502

[14] Muller C, Ferenczi T A M, Campoy-Quiles M, Frost J M, Bradley D D C, Smith P, Stingelin-Stutzmann N and Nelson J 2008 *Adv. Mater.* **20** 3510

[15] Baek W, Yoon T, Lee H H and Kim Y 2010 *Org. Electron.* **11** 933

[16] Li G, Shrotriya V, Huang J, Yao Y, Moriarty T, Emery K and Yang Y 2005 *Nat. Mater.* **4** 864

[17] Yao Y, Hou J H, Xu Z, Li G and Yang Y 2008 *Adv. Funct. Mater.* **18** 1783

[18] Ouyang J Y and Xia Y J 2009 *Sol. Energy Mater. Sol. Cells* **93** 1592

[19] Jeong J W, Huh J W, Lee J I, Chu H Y, Han I K and Ju B 2010 *Curr. Appl. Phys.* **10** S520

[20] Clarke T M, Ballantyne A M, Nelson J, Bradley D D and Durrant J R 2008 *Adv. Funct. Mater.* **18** 4029

[21] Miller S, Fanchini G, Lin Y, Li C, Chen C, Su W and Chhowalla M 2008 *J. Mater. Chem.* **18** 306

[22] Li G, Yao Y, Yang H, Shrotriya V, Yang G and Yang Y 2007 *Adv. Funct. Mater.* **17** 1636

[23] Campoy-Quiles M, Ferenczi T, Agostinelli T, Etchegoin P G, Kim Y, Anthopoulos T D, Stavrinou P N, Bradley D and Nelson J 2008 *Nat. Mater.* **7** 158

[24] Germack D S, Chan C K, Kline R J, Fischer D A, Gundlach D J, Toney M F, Richter L J and Delongchamp D M 2010 *Macromolecules* **43** 3828

[25] Parnell A J, Dunbar A D, Pearson A J, Staniec P A, Dennison A J, Hamamatsu H, Skoda M W, Lidzey D G and Jones R 2010 *Adv. Mater.* **22** 2444

[26] Kiel J W, Kirby B J, Majkrzak C F, Maranville B B and Mackay M E 2010 *Soft Matter* **6** 641

[27] Pavlopoulou E, Fleury G, Deribew D, Cousin F, Geoghegan M and Hadziioannou G 2013 *Org. Electron.* **14** 1249

[28] Ruderer M A, Guo S, Meier R, Chiang H, K O Rstgens V, Wiedersich J, Perlich J, Roth S V and Ller-Buschbaum P 2011 *Adv. Funct. Mater.* **21** 3382

[29] Germack D S, Chan C K, Hamadani B H, Richter L J, Fischer D A, Gundlach D J and Delongchamp D M 2009 *Appl. Phys. Lett.* **94** 233303

[30] Xue B, Vaughan B, Poh C, Burke K B, Thomsen L, Stapleton A, Zhou X, Bryant G W, Belcher W and Dastoor P C 2010 *J. Phys. Chem. C* **114** 15797

[31] Brabec C J, Heeney M, Mcculloch I and Nelson J 2011 *Chem. Soc. Rev.* **40** 1185

[32] Skriver H L and Rosengaard N M 1992 *Phys. Rev. B* **46** 7157

[33] Loiudice A, Rizzo A, Latini G, Nobile C, de Giorgi M and Gigli G 2012 *Sol. Energy Mater. Sol. Cells* **100** 147